CryoSat Instrument Performance and Ice Product Quality Status

Jerome Bouffard [(1)], Erica Webb[(2)], Michele Scagliola[(3)], Albert Garcia-Mondéjar[(4)], Steven Baker[(5)], David Brockley[(5)], Julia Gaudelli[(5)], Alan Muir[(5)], Amanda Hall[(2)], Rubinder Mannan[(2)], Mònica Roca[(4)], Marco Fornari[(1)], Pierre Féménias[(6)] and Tommaso Parrinello[(6)]

(1) RHEA c/o ESA, Earth Observation Directorate, 2 Via Galileo Galilei 2, 00044 Frascati – Italy *Mail: Jerome.bouffard@esa.int ; Tel: +39 06 9418 8435
(2) Telespazio VEGA UK Ltd, 350 Capability Green, Luton, Bedfordshire LU1 3LU, UK
(3) Aresys, via Privata Flumendosa, 16, 20132 Milan, Italy
(4) isardSAT, Surrey Space Incubator, 40 Occam Road, The Surrey Research Park, Guildford, UK
(5) MSSL-UCL, Holmbury House, Holmbury St Mary, Dorking, Surrey, RH5 6NT, UK
(6) ESA, Earth Observation Directorate, Via Galileo Galilei, 2 –00044 Frascati, Italy

Abstract:

Over the past 20 years, satellite radar altimetry has shown its ability to revolutionise our understanding of the ocean and climate. Previously, these advances were largely limited to ice-free regions, neglecting large portions of the Polar Regions. Launched in 2010, the European Space Agency's (ESA) polar-orbiting CryoSat satellite was specifically designed to measure changes in the thickness of polar sea ice and the elevation of the ice sheets and mountain glaciers. To reach this goal, the CryoSat products have to meet the highest performance standards, achieved through continual improvements of the associated Instrument Processing Facilities. Since April 2015, the CryoSat ice products are generated with Baseline-C, which represented a major processor upgrade. Several improvements were implemented in this new Baseline, most notably the release of freeboard data within the Level 2 products. The Baseline-C upgrade has brought significant improvements to the quality of Level-1B and Level-2 products relative to the previous Baseline-B products, which in turn is expected to have a positive impact on the scientific exploitation of CryoSat measurements over land ice and sea ice. This paper provides an overview of the CryoSat ice data quality assessment and evolutions, covering all quality control and calibration activities performed by

ESA and its partners. Also discussed are the forthcoming evolutions of the processing chains and improvements anticipated in the next processing Baseline.

Key words: CryoSat, Altimetry, Cryosphere, ice product status, Instrument performance, long-term stability, ice product evolutions

1 Introduction

As the effects of a fast-changing climate are becoming apparent, it is increasingly important to understand how the Earth's cryosphere is responding, particularly in the Polar Regions. Diminishing ice cover is frequently cited as an early casualty of global warming and since ice, in turn, plays an important role in regulating climate and sea level, the consequences of this change are far-reaching. To better understand how climate change is affecting these remote and sensitive regions, there remains an urgent need to determine more precisely how the thickness of the ice is changing, both on land and floating on the sea.

In this respect, the European Space Agency's (ESA's) Earth Explorer CryoSat-2 (hereafter CryoSat) was launched on 8th April 2010. The primary mission objectives are the determination of the regional and basin-scale trends in perennial Arctic sea ice thickness and the contributions that the Antarctic and Greenland ice sheets make to global sea level changes. The secondary mission objectives are the observation of the seasonal cycle and variability of Arctic and Antarctic sea ice mass and thickness in addition to the variation in thickness of the Earth's ice caps and glaciers. By addressing these challenges, the data delivered by CryoSat can be used to better understand the role ice plays in the Earth system (Wingham et al. 2006; Parrinello et al. 2017, introduction of this Special issue). Beside its ice-monitoring objectives, CryoSat also provides valuable measurements for ocean scientific and operational applications (Calafat et al., 2017; Bouffard et al., 2017, this issue).

The CryoSat data are processed by ESA over both ice and ocean surfaces using two independent processors, generating a range of operational products with specific latencies. The Ice processor generates Level 1B (L1B) and Level 2 (L2) offline products typically 30 days after data acquisition for the three instrument modes: Low Resolution Mode (LRM), Synthetic Aperture Radar (SAR) and SAR Interferometric (SARIn). Fast Delivery Marine (FDM) products are generated in Near Real Time (NRT) from LRM data and distributed 2-3 hours after acquisition. The ice products are currently generated with the Baseline-C Ice processors. CryoSat ocean data are generated with the Baseline-B CryoSat Ocean Processor (more details in Bouffard et al., 2017, this issue). In order to achieve the highest quality data products, and meet mission requirements, the CryoSat Ice and Ocean processing chains are periodically updated. Processing algorithms and associated product content are regularly improved based on internal and external recommendations from the scientific community, Expert Support Laboratories, Quality Control Centres and validation campaigns (Figure 1).

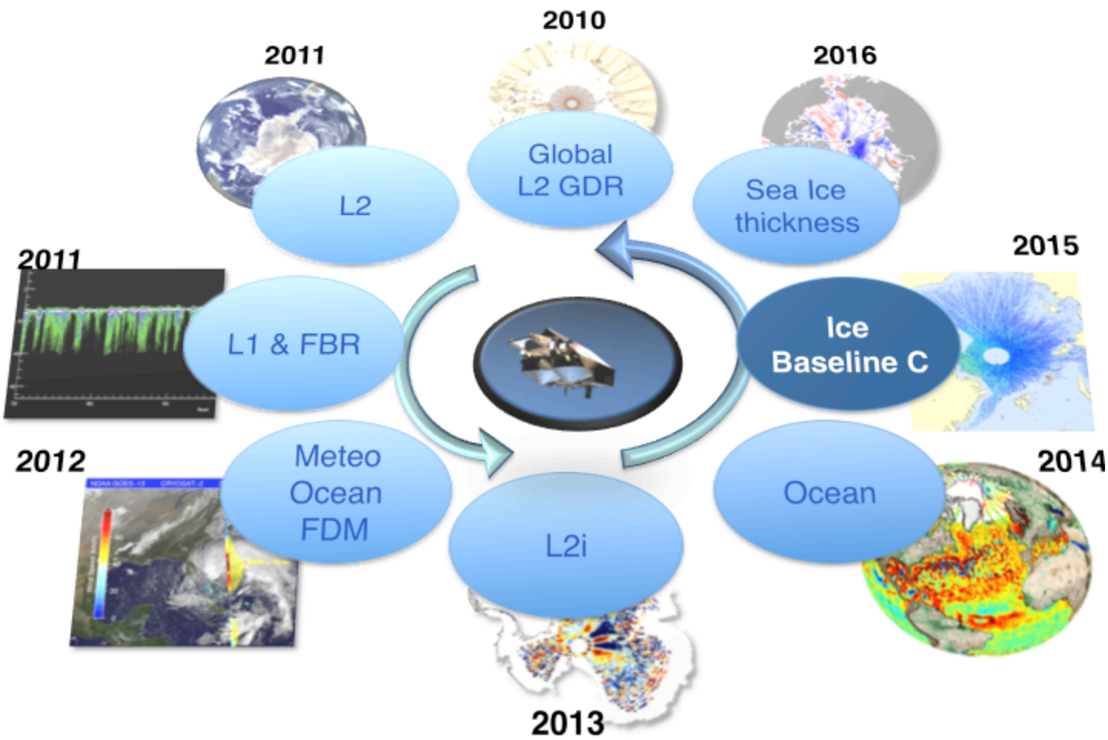

Figure 1: Overview of CryoSat Product Evolution over the past 7 years.

The CryoSat Baseline-C ice products are routinely monitored for quality control by the ESA/ESRIN Sensor Performance, Products and Algorithms (SPPA) office with the support of the Instrument Data quality Evaluation and Analysis Service (IDEAS+). Calibration products are also routinely monitored to check the quality of corrections applied to operational L1B products and verify the long-term status of the satellite's instrument: the Synthetic Aperture

Interferometric Radar Altimeter (SIRAL). Data acquired over transponders are also used to perform external calibrations of the SIRAL. The quality of the final ice products is then monitored and analysed.

This paper provides an overview of the CryoSat ice product quality status and evolutions. After briefly presenting the CryoSat Ice processing baselines, the paper focuses on ESA activities and results of internal and external calibrations, quality control and quality analysis. Also discussed are the forthcoming evolutions of the processing algorithms, geophysical corrections and validation approaches to accommodate future upgrades to the CryoSat Ice processing chains. This paper is complementary to Bouffard et al. (2017, this issue) focusing on the CryoSat quality control, validation and product evolutions of the CryoSat ocean products.

2 CryoSat Ice Processing Chains

2.1 Ice Processor Historic Baselines

CryoSat was designed to measure changes in polar sea ice thickness and ice sheet elevation. To reach this goal the CryoSat data products have to meet the highest performance standards and are subjected to a continual cycle of improvement, achieved through upgrades to the processing chains. The most recent major upgrade of the CryoSat Ice processing chains took place in April 2015, with the release of Baseline-C. Prior to Baseline-C, two major product Baselines (A and B) had been released to users since the launch of the mission and the first CryoSat Reprocessing Campaign was completed in December 2013.

The change from Baseline-A to Baseline-B was primarily motivated by the need to improve the performance of CryoSat over sea ice. Baseline-B was implemented into operations and used to generate CryoSat products from February 2012 onwards. The main improvement introduced in Baseline-B with respect to Baseline-A was the application of a range oversampling by a factor of 2 to the 20 Hz SAR/SARIn waveforms. This allowed the aliasing of the signal when the square-law detection is applied to be avoided but, in order to fit the double length waveform in the L1B product files, a truncation of the trailing edge of the waveform was needed. An improved L2 SAR discriminator and tuned retracker thresholds were also implemented and several configuration parameters were improved. An FDM processor was first introduced in Baseline-B to generate products with an average latency of 2-3 hours.

The FDM product was improved in April 2013 with the implementation of an upgraded processor. The main evolutions comprised the tuning of the FDM retracker thresholds and the backscatter coefficient calculated from an improved algorithm developed by the National Ocean and Atmospheric Administration (NOAA). Additionally, the Global Ionospheric Map correction and meteorological forecast auxiliary data files were used in the NRT processing chains. Several FDM configuration parameters were improved to generate FDM L2 data with a quality comparable to other ocean-oriented altimetry missions (more details in Bouffard et al. 2017, this issue). The Baseline-B processors were used in the first CryoSat Reprocessing Campaign to reprocess all offline ice data (LRM, SAR and SARIn) back to the start of the mission (July 2010).

Baseline-C represents a major upgrade to the CryoSat Ice processing chains and introduces several evolutions with respect to Baseline-B. It is also the baseline used for the second CryoSat Reprocessing Campaign. The Baseline-C upgrade concerns both the L1 and L2 processing chains, bringing significant improvements to the quality of data products over land ice and sea ice, relative to the previous Baseline-B products.

Before being implemented into operations, several test datasets were generated with the new processors to check the quality of data products and to validate that all anomalies for which solutions have been implemented, have in fact been successfully resolved and that no new problems have arisen as a result. The first test dataset chosen for this validation was the 21^{st} – 23^{rd} August 2011, which is the period chosen initially for the first CryoSat validation since it comprised a period of complete, good quality data. This same period has been used in all subsequent CryoSat validations to enable non-regression testing to be performed. All new test data is checked in comparison to test data generated using the previous processing chain, in order to ensure that intended changes have occurred and that no other, unintended changes to the product quality have arisen. All products are checked against the updated product format specifications, delivered with the updated processors, to ensure that any format changes and content changes are expected. The second test dataset selected for this validation covered the period 8th – 14th November 2010 and was chosen specifically for the analysis and verification of freeboard values in the L2 SAR products, selected from a month when high concentrations of sea ice were experienced in the Arctic.

For the majority of anomaly reports, it was possible to verify whether the anomaly had been successfully fixed through detailed analysis of the products in the two main test datasets. However, if an anomaly report related to a product or problem which fell outside of the test dataset coverage, then additional test data was generated specific to each case, and used to verify whether a solution had been successfully implemented. In total 30 anomaly reports were successfully resolved and verified in the Baseline-C validation.

2.2 Ice Baseline C processor upgrades

Following a successful validation, the new processors were approved and implemented into operations at the Payload Data Segment. Since April 2015, the CryoSat ice products have been generated with the new Baseline-C Ice processing chains. A few of the major changes are described below. A complete list of the evolutions and changes implemented in Baseline-C can be found in the technical notes section of the CryoSat Wiki page (https://wiki.services.eoportal.org/tiki-index.php?page=CryoSat%20Wiki).

- Power normalisation in SAR and SARIn: In Baseline-B the peak power of the 20 Hz L1B waveforms for SAR and SARIn was too high. In Baseline-C the power scaling has been corrected and the peak power values are now as expected, according to the sigma-0 of the sea surface (Scagliola et al., 2015).

- Attitude information in L1B products: In Baseline-C a new Star Tracker Processor was developed to create files containing the most appropriate Star Tracker data. These files are used in offline processing only. In addition, new fields were added to the L1B products to include the antenna bench angles (roll, pitch and yaw) and the sign conventions of these fields were updated.
- Datation and range biases in L1B: Several sources of datation and range biases were identified in the Baseline-B L1B products for all modes. In particular, the datation biases were reduced, improving the on-ground decoding of the timestamps of instrument source packets. The range biases were reduced for all the modes by a post-launch update of the fixed instrument path delay and of the position of the centre of mass of the spacecraft. Additionally, for LRM only, a one-gate shift due to the on-board definition of fast Fourier transform was identified and taken into account in the Baseline-C ground processing. These biases were largely resolved in Baseline-C L1B products as shown by external calibration results at the Svalbard transponders (see Section 3.4.3).
- New retracker for land ice (LRM): A new Land Ice Retracker was developed and implemented by University College London (UCL). The Land Ice Retracker follows the typical method for a retracker that fits a Brown (1977) model to the LRM waveform. The iterative model fit is initialised with the Offset Centre of Gravity (OCOG) retracker (a threshold retracker). The Land Ice Retracker provides an alternative to the existing Customer Furnished Item (CFI) retracker and can be tuned as necessary in the future to improve performance.
- Arctic Mean Sea Surface (MSS) for SAR: A new Arctic MSS (UCL13) was created, using CryoSat data to provide improved resolution and coverage over Polar Regions. UCL13 was specifically designed to improve the computation of the interpolated Sea Surface Height Anomaly (see Skourup et al., 2017, and Ridout, 2014). The new UCL13

MSS combines (via a linear merge from 50ºN-60ºN) the existing Collecte Localisation Satellites 2011 (CLS2011) model with CryoSat Arctic data in order to provide full coverage over the Arctic Ocean (see Figure 2).

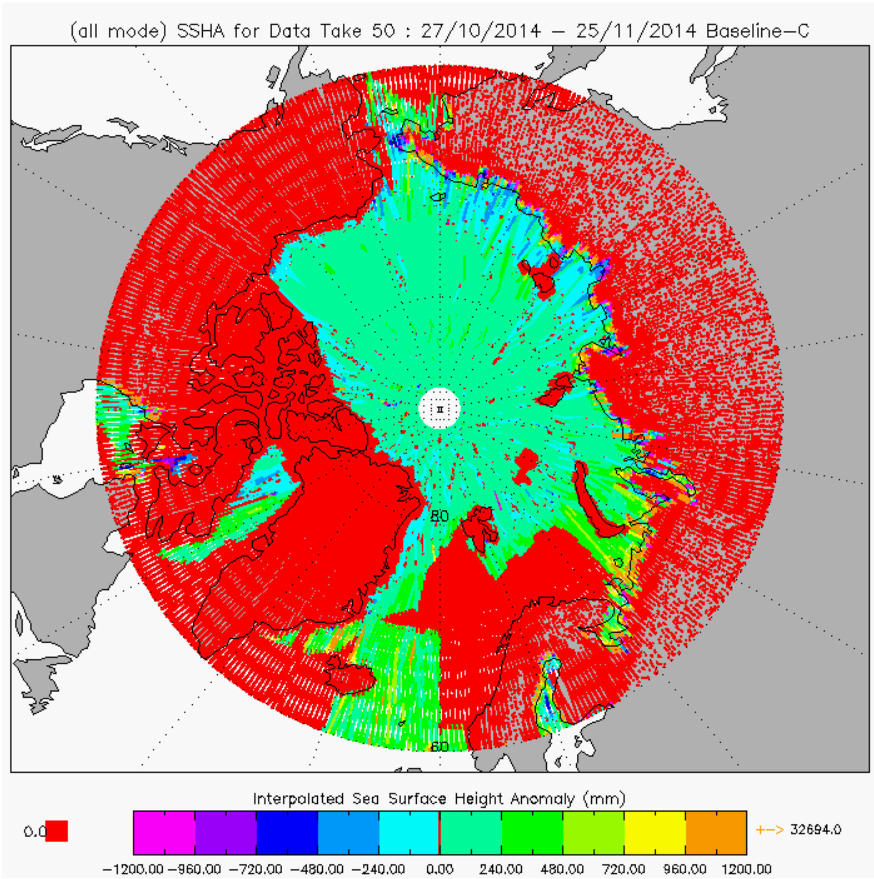

Figure 2: Sea Surface Height Anomaly, Arctic, 27/10/2014 - 25/11/2014

- Retracker improvement and freeboard activation for SAR (see Bouzinac, 2012): Freeboard values are now computed in the L2 SAR products following the introduction of the new UCL3 MSS. The SAR retracker was improved and adapted for diffuse echo returns from open ocean and sea ice floes. Initial analysis of freeboard confirms expected results and geographical distribution (see Figure 3, Section 2.4 and Section 3.4 for more details).

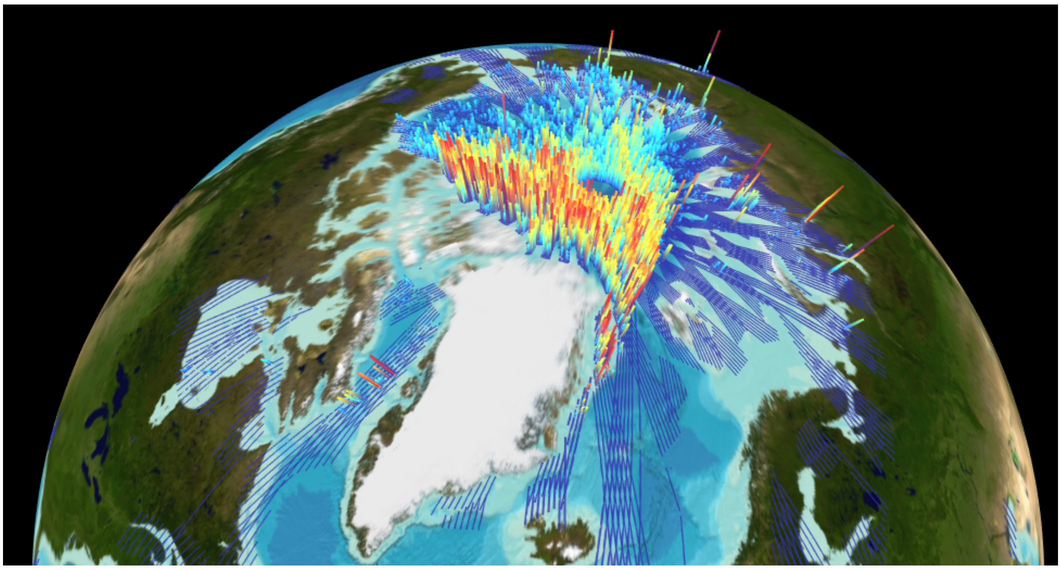

Figure 3: Freeboard values (scale: blue: 0 m - red: 1 m) for the Arctic region, plotted for 15 days of Baseline-C L2 SAR data (01/01/2017 - 15/01/2017). Map plotted with the VtCryoSat© tools (http://visioterra.net/VtCryoSat/).

- New Digital Elevation Model (DEM) for SARIn: New higher resolution DEMs for Antarctica (Bamber, 2009, 1 km resolution) and Greenland (Greenland Ice Mapping Project, 500 m resolution) were implemented at Baseline-C. For heights derived from SARIn phase differences, a DEM is used to check whether a phase-wrapping ambiguity may have occurred and set a warning flag. Previous DEMs proved to be inaccurate at the ice sheet margins resulting in frequent and erroneous settings of the SARIn ambiguity flag and the cross-track angle error flag. At Baseline-C, the new DEMs resolve most of these false errors and many more retracked waveforms are now flagged as valid in the L2 ice products.

2.3 Main Level 1 Processing steps

Level 0 (L0) to L1B processing is aimed at generating the L1B products which contain geo-located, instrument calibrated and multilooked waveforms at ~20 Hz rate. While LRM and SAR L1B products contain only multilooked power waveforms, SARIn L1B products contain multilooked power, interferometric phase difference and coherence waveforms. The CryoSat L1B processing chain is continuously maintained and upgraded.

A functional view of the SAR/SARIn L1B processing chain is given in Figure 4. For a detailed description of the L0 to L2 processing chain refer to Cullen et al. (2007).

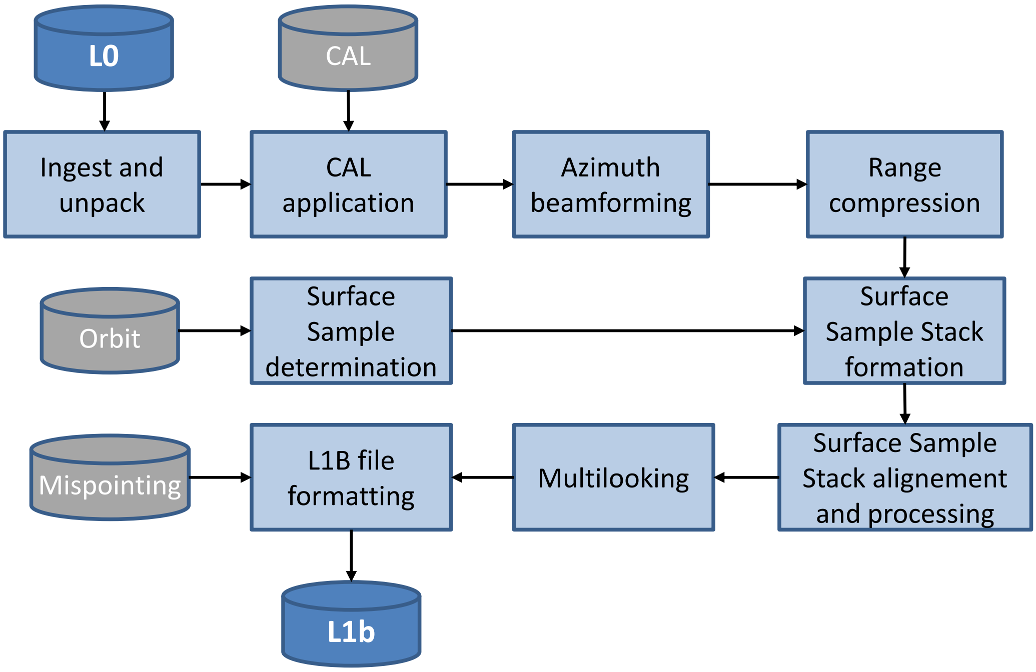

Figure 4: SAR/ SARIn L0 to L1B processing chain

By inspection of Figure 4, the following processing steps for SAR/ SARIn are identified:

- Ingest and unpack: instrument source packets are unpacked, decoded and converted to engineering units. The echoes for each mode are copied across.
- Calibration application: the instrument calibration corrections are applied to echoes. For more details on the SIRAL calibration corrections see Section 3.2. The Baseline-C L1 processing chain improved the application of the Calibration 1 (CAL1) corrections by correctly applying the power gain correction in all modes and the pulse-to-pulse amplitude correction in SAR/ SARIn mode (Scagliola et al., 2015).

- Surface sample determination: this step determines the set of on-ground surface locations where the synthesised Doppler beams are directed. The surface sample determination is based on an iterative method that places the surface sample on the ground elevation profile with a fixed angular separation along-track, resulting in a posting rate of about 20 Hz.
- Azimuth beam-forming: each burst, which is composed by 64 phase coherent echoes, undergoes a fast Fourier transform in the along-track direction to synthesize 64 Doppler beams that are equally spaced in angle and pointed to 64 different locations on the ground. The sharpening of the Doppler beams results in an improved along-track resolution.
- Range compression: this step is implemented by a fast Fourier transform in the delay direction of each echo. In SAR/ SARIn mode, the echoes are zero-padded prior to performing the range compression so that the waveform length is doubled. The Baseline-C L1 processing chain was improved to accommodate the whole range window for the oversampled waveforms in the SAR/ SARIn L1B product, see Scagliola et al. (2015).
- Surface sample stack formation: the single look waveforms corresponding to all Doppler beams pointed to a given surface sample are arranged in a surface sample stack matrix, one for each receiving chain in SARIn mode. This way, all the statistically independent looks generated by the different bursts, for a given surface location on the ground, are gathered.
- Surface sample stack alignment and processing: this step is aimed at compensating all the range misalignments among the single looks in a surface sample stack: slant range migration correction, window delay alignment and Doppler range correction. In Baseline-C, the slant range migration correction is moved from burst level to stack level in order to increase the quality of waveforms in acquisitions with a high altitude rate (see Scagliola et al., 2015). Furthermore, the Baseline-C L1 processing chain applies a surface sample stack weighting that allows the filtering out of the single looks originated

by the furthest acquired bursts with respect to the surface sample, resulting in an improved signal-to-clutter-noise ratio on the multilooked waveforms (Scagliola et al., 2015).

- Multilooking: multilooking is the incoherent averaging of all the power single looks in a surface sample stack. The result is the multilooked power waveform for the on-ground surface location. Additionally, in the case of SARIn mode only, the multilooked phase difference and the coherence waveforms are computed too.
- L1B file formatting: the L1B product file is generated providing the geo-located calibrated waveforms with all the ancillary information according to the product format specifications. Major modifications were implemented in Baseline-C to improve the quality of the mispointing angles in L1B products (Scagliola et al., 2015). In particular, pitch and roll biases are compensated for in Baseline-C L1B products and the mispointing angles are computed from the same Star Tracker that is selected on board, as these are the best available Star Tracker at a given time.

2.4 Level-2 Processing steps

Further details on the L2 processing scheme used for each mode, such as the retrackers, can be found in the CryoSat Product Handbook (Bouzinac, 2012). The L2 processing scheme follows the main steps described here below, in order deduce the ice elevation over land ice margins and interior, and freeboard values over sea ice regions (Figure 5).

- L1B data is ingested and the flags are checked. Data flagged as bad at L1B is not processed further, but is output to L2 in its current form (to retain a 1:1 relationship between L1B and L2 data).
- Auxiliary data, such as snow depth and sea ice concentration, are merged into the product, following interpolation from auxiliary files based on position and time.

- Surface type and echo type discriminations are performed. This determines the type of retracking to be performed and the set of geophysical corrections to use, or flags the waveform as unusable.
- The appropriate set of geophysical corrections are applied to the range determined by the on-board tracker,
- Retracking is performed. The methods used are mode and surface type dependent. In the case of SARIn data, the phase and coherence waveforms are also processed. The elevation is computed, accounting for the estimated location of the echoing point. This may be derived via a slope model for LRM.
- Over the steep slopes of the ice-sheet margins (where the SARin mode is used), it is possible that the geolocation of the echoing point has been affected by phase-wrapping. This can place the echoing point on the wrong side of the nadir track, and will result in a significant (~60 m) error in height estimation. A reference DEM is used to flag points that have potentially been affected, however, it is important to note that it may be the DEM that is incorrect, not the measurement.
- For the smoothly sloping ice-sheet interior (where LRM is used), it is possible to pre-compute the expected echoing location by use of a range-slope model derived from a DEM. This slope model allows the retrieval of the echo-location based on the nadir position; the height at that position can then be computed via trigonometry from the measured range.
- For sea ice regions (where SAR mode is used), during the creation of the continuous sea surface height anomaly parameter, the height anomaly must be interpolated for records where it cannot be directly measured, i.e. records where sea ice has been detected. This interpolation is performed using a linear interpolation of the available measurements within the Rossby radius of the measurement point. The freeboard measurement is then computed by subtracting this interpolated sea surface height.

- The computed L2 geophysical parameters and supporting L1B values are then packaged and output as L2 and Level 2 In-depth (L2i) products

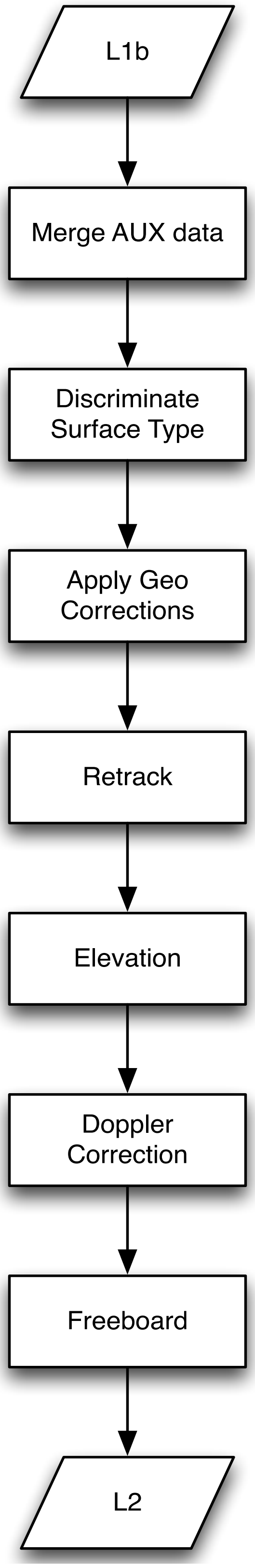

Figure 5: Main L2 processing steps

3 CryoSat Data Quality Assessment

3.1 Routine Quality Control

3.1.1 Background

Since the launch of CryoSat in 2010, IDEAS+ has routinely assessed the performance and quality of the CryoSat data products, and provided support to investigations and user queries. Since August 2008 IDEAS+ has provided an operational quality control service to ESA for both ESA-owned Earth Observation missions and Third Party Missions. IDEAS+ provides support throughout the development and validation of new ESA operational processing chains. IDEAS+ is also heavily involved in CryoSat reprocessing campaigns, providing support during configuration of the reprocessing facility, and subsequently checking all reprocessed data before it is released to the scientific and user community.

3.1.2 Material and Methods

IDEAS+ performs routine quality control activities on all operational CryoSat products, which includes checking L0 data availability; the acquisition tracking and L0 echo errors; the product headers; the product formats and software versions; the auxiliary data file usage; the external correction error flags and the analysis of measurement parameters.

IDEAS+ uses a number of different tools and software to perform their operational analyses. The CryoSat 2 Quality Control – Quality Analysis of Data from Atmospheric Sensors (C2QC-QUADAS) is an updated tool installed in April 2015 at the Payload Data Segment, the Centre for Environmental Monitoring from Space, and on local machines at Telespazio Vega UK. It is configured to monitor both operational and reprocessed ice and ocean data products, and to automatically generate daily and monthly quality control reports, which form the basis of the IDEAS+ daily performance reports. The Quality Control for CryoSat (QCC) tool is installed at the Payload Data Segment and is designed to perform a set of configurable checks on each product immediately after production. This information is checked and included in the IDEAS+ daily performance reports.

3.1.3 Results

IDEAS+ perform daily routine quality control checks on all operational CryoSat products. Quality Control Performance Reports summarising these checks are uploaded daily to the ESA CryoSat webpage (https://earth.esa.int/web/guest/missions/esa-operational-eo-missions/cryosat/daily-performance-reports). Incorporated into these reports are outputs from the QCC tool integrated at the ESA Payload Data Segment. The QCC tool performs error and warning checks for all L1B, L2 and L2i CryoSat products according to a pre-defined Test Definition File. The warning tests check that specific parameters and geophysical corrections fall within expected thresholds or are set to certain values. Every time a value in a product exceeds the thresholds, a warning is recorded in the QCC report for that product. The initial test thresholds were defined at the beginning of the mission using early experience of expected values from other altimetry missions. As no deep analysis was performed for these thresholds, it was always intended that they would be updated once the mission was more established.

In 2016 IDEAS+ performed detailed analysis of each field included in the QCC CryoSat product checks in order to update and tune these test thresholds. The values of all products from June and December 2014 were plotted along with the current thresholds. If a large percentage of the data exceeded the thresholds, i.e. not only extreme values, new thresholds were identified. Statistical analysis was performed on all Baseline-B L1B and L2 ice products from June and December 2014. Analysis involved extracting the mean ± 3 standard deviations, maximum and minimum values from the test data for each QCC test. If the data had a normal distribution, the mean ± 3 standard deviations was used to set the new thresholds. Where the data did not have a normal distribution, each test was assessed on a case by case basis, using knowledge from other missions were appropriate, to identify the most suitable thresholds. The new recommended thresholds should therefore better encompass the expected values and to improve the flagging of outliers.

For example, the original threshold used to check the altitude of the satellite Centre of Gravity (COG) (the ‘RangeAltitudeCOG’ test) was set at 700 to 750 km, meaning that all sample values must fall within these thresholds otherwise the product will be flagged with a warning. In Baseline-B, i.e. before the threshold update, this flag was raised for approximately 20% of all L1B and L2 products. Based on our analysis it was decided to adjust the thresholds to 710 to 760 km in order to ensure that the expected data values pass the test and only the extreme outliers are flagged.

With the release of Baseline-C data it has been possible to assess the suitability of the updated thresholds for the altitude test. Figure 6 shows the monthly mean ± 1 standard deviation (black dots and bars), maximum (purple crosses) and minimum (blue crosses) values from January 2013 – February 2016. The ± 3 standard deviation range is shown by the grey shaded area.

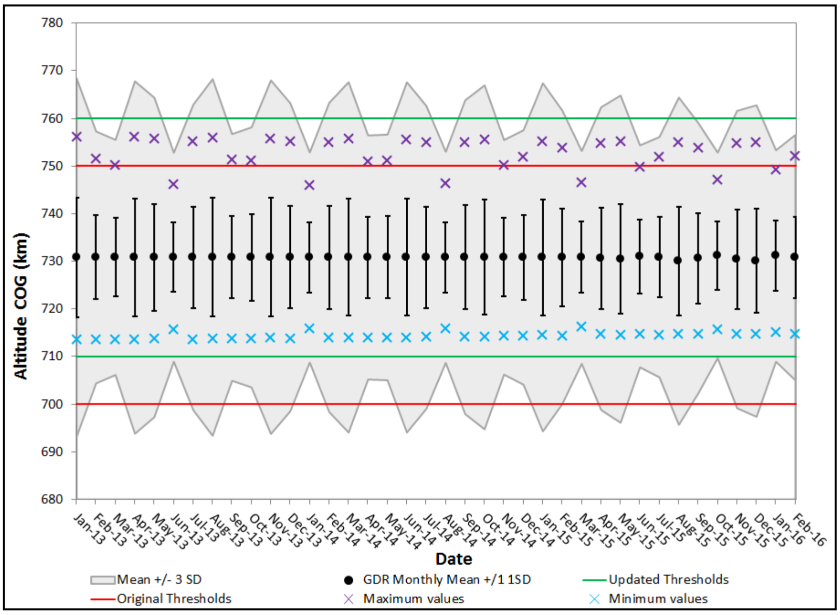

Figure 6: Time series of altitude relative to the satellite Centre of Gravity from Baseline-C data, from January 2013 to February 2016.

It is clear from the original thresholds (in red) that the upper threshold would have flagged a number of products each month that have high values, but that the lower threshold was too far from the expected data range to flag unexpected values. As altitude does not have a normal distribution, using the standard deviation to derive the new thresholds was not suitable. The agreed new thresholds (in green) now better encompass the expected altitude values, but should flag extreme or unexpected values.

The new thresholds for all L1/L2 parameters were then implemented in an updated delivery of the QCC software and installed into operations at the CryoSat Payload Data Segment. So far daily analysis of the QCC results indicates that the new QCC thresholds are more appropriate. Long-term analysis of Baseline-C data will highlight whether the thresholds need to be amended in future.

3.2 SIRAL Internal Calibrations Monitoring

3.2.1 Background

The calibration strategy for SIRAL includes both internal calibrations and external calibrations (see Section 3.3 and Fornari et al., 2014). The internal calibrations are performed on the instrument and the measurements obtained by SIRAL are transmitted to the ground. The calibration L0 data are processed on the ground and the resulting calibration corrections are used to calibrate the science products for the SIRAL instrument (Cullen et al., 2007). According to Scagliola et al. (2015), all the calibration corrections are applied to science products in Baseline-C L1B products. Furthermore, as already shown in Scagliola et al. (2016), the calibration corrections can be used to monitor the performance of the SIRAL instrument over the long term. In fact the calibration products, which have been designed to measure the actual characteristics of the instrument and to compensate for them on the ground, can be analysed to highlight how the instrument behaviour is changing over time, due to its thermal status (see section 3.2.3) or potential on-board software or hardware anomalies.

Since 2012, Aresys has provided continuous support for the quality monitoring of the calibration corrections contained in the corresponding calibration products. In particular, the calibration products are routinely monitored in order to produce offline L1B science data using only validated calibration corrections. On the other hand, the calibration corrections are monitored over the long term with the aim of verifying the instrument performance during the mission lifetime.

3.2.2 Material and Methods

SIRAL is a phase coherent pulse-width limited radar altimeter with interferometric capabilities. To support its novel operating modes, additional calibration paths are implemented on-board to obtain the calibration corrections on-ground. These are necessary to correct for the transfer function phase with respect to frequency and for the phase difference between the two receiving antennas. Periodic instrument calibrations are performed in flight in order to correct the science products for instrument distortions. The calibrations are periodically performed on a time or zone basis, depending on the calibration.

The following internal calibration sequences are regularly commanded on SIRAL:

- The CAL1 to calibrate the internal path delay and the peak power by measuring the range impulse response for all the SIRAL modes. Moreover, for SAR and SARIn modes only, the variations in gain and phase between successive pulses in a burst are measured. By analysis of the range impulse response it is possible to evaluate its peak-to-side lobe ratio and -3 dB width, which are quality parameters for the instrument impulse response. The CAL1 is commanded each time CryoSat passes over a defined zone in Asia, resulting in a repeat frequency of between one and two times per day.
- The Complex Calibration 1 (CCAL1), also named AutoCAL, to calibrate the Automatic Gain Control and Analog-to-Digital Converter for gain and phase difference between the two receiving chains. The CCAL1 is commanded each time CryoSat

passes over a defined zone in the Sahara, resulting in a repeat frequency of between one and two times per day.

- The Calibration 2 (CAL2) to evaluate the instrument transfer function across the measurement spectrum. The CAL2 is commanded twice a month.
- The Calibration 4 (CAL4) to calibrate the interferometer for the phase difference between the two receiving chains. The CAL4 is interleaved in the SARIn measurements and is commanded once each second. It is worth noting that both CCAL1 and CAL4 measure the phase difference between the two receiving chains but, the CCAL1 calibrates only the signal paths in the digital and radio frequency instrument sections (Rey et al., 2001). The CAL4 also includes the transmission amplifier and duplexer.

The time frequency of the calibrations listed above are determined by the calibration plan that has been adopted since March 2011. For more details on the SIRAL internal calibrations, please refer to Scagliola et al. (2016).

The long-term analysis of the calibration corrections can be used to monitor the performance of the SIRAL instrument starting from the beginning of the operational phase of the CryoSat mission. The calibrations corrections are analysed by exploiting ad-hoc developed tools in order to verify the following points:

- Whether the calibration corrections are changing as function of the time. In particular, the linear trend in the corrections is measured, in order to assess the changing rate of the correction as function of time. It is useful to have a rough prediction of the behaviour of the SIRAL instrument with age as it may have an impact on the instrument performance and, in turn, mission performance.
- Whether the calibration corrections depend on the thermal status of the instrument. Largely due to the non-sun-synchronous orbit of CryoSat, the temperature of the spacecraft changes both in the short term, as a function of the orbit period, and on the long term, as a function of the relative position with respect to the sun, which has a

period of about 480 days. By joint analysis of the instrument characteristics, continuously tracked by the internal calibrations, and of the instrument temperatures, it has been verified that the thermal status of the SIRAL affects the instrument behaviour both in the short and long term.

- Whether the calibration corrections depend on the ascending/descending orbit, for the calibrations that are commanded when CryoSat passes over a defined zone. Actually, the calibration corrections are always dependent on the thermal status of the instrument, which differs depending on whether the orbit is ascending or descending due to the different sun illumination.

It is worth remarking here that the internal calibrations allow characteristics of SIRAL to be tracked continuously. Therefore, applying the calibration corrections to the science data means that the variability of the instrument (as a function of time and thermal status) is already compensated for in the CryoSat L1B products. In the following section, some results from the analysis of the CryoSat calibration corrections are shown.

3.2.3 Results

Figure 7 displays the calibration corrections applied to science data for SAR mode; similar behaviours have been observed for the other modes. The corrections are shown from November 2010 to November 2016. By inspection of Figure 7(a) it can be observed that the gain variation correction has been increasing with an approximately constant trend from the beginning of the mission, which in turn causes a decrease of the signal-to-noise ratio of about 1.2 dB from November 2010. It should be noted that this behaviour was expected during the operational life of SIRAL, and is similar to trends observed for other pulse-limited altimeters. Moreover, it can be noticed that the corrections are denser up to February 2011 since, in that period, a different calibration plan was used. In Figure 7(b) the internal path delay correction is shown and a slight increasing trend in the corrections can be observed the time. In Figure

7(c) and Figure 7(d) the pulse-to-pulse amplitude and the pulse-to-pulse phase correction are shown respectively. Their behaviour has been stable from beginning of the operational phase. Only the pulse-to-pulse phase correction has had small evolutions up to 2011 and exhibits some periodical variations related to the SIRAL temperature.

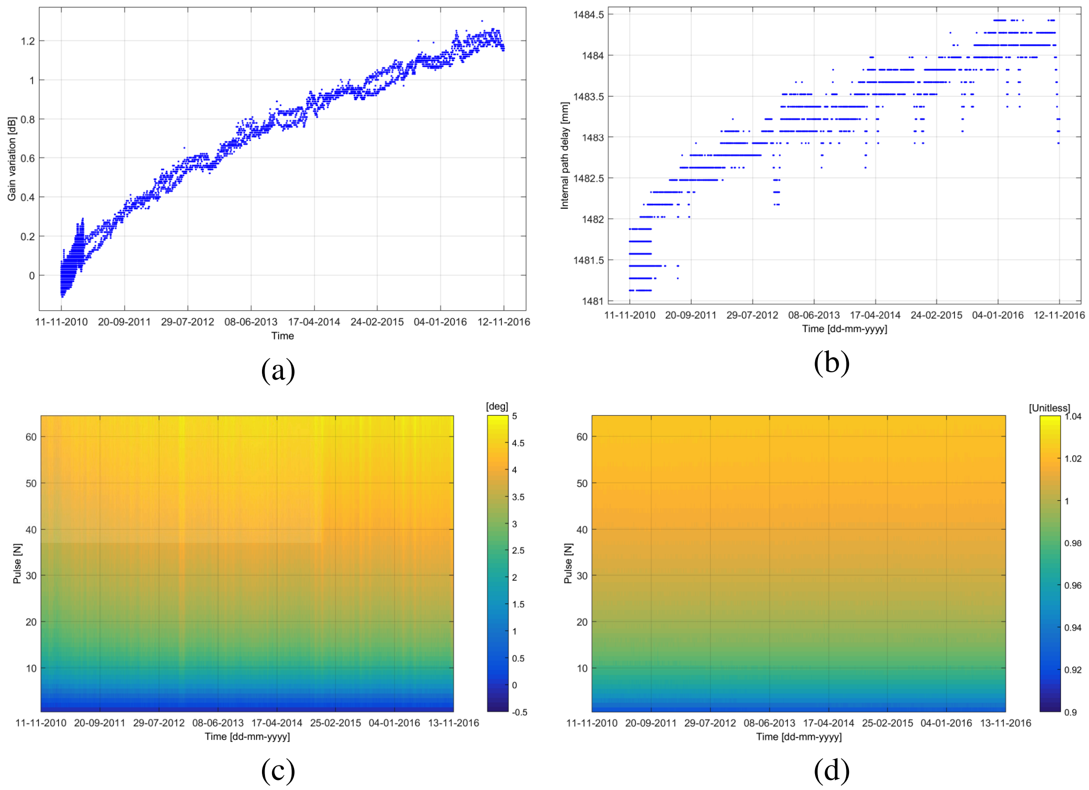

Figure 7: CAL1 SAR calibration corrections: gain variation (a), internal path delay (b), pulse-to-pulse amplitude (c) and pulse-to-pulse phase (d).

In Figure 8, the gain variation corrections for CAL1 SAR are shown, highlighting the corrections obtained during ascending or descending passes over the calibration zone. By inspection of Figure 8 it can be observed that, depending on the period, the calibration corrections for the different orbit directions can differ by up to 0.1 dB. This difference was mainly due to the different thermal status of the instrument as function of the orbit direction.

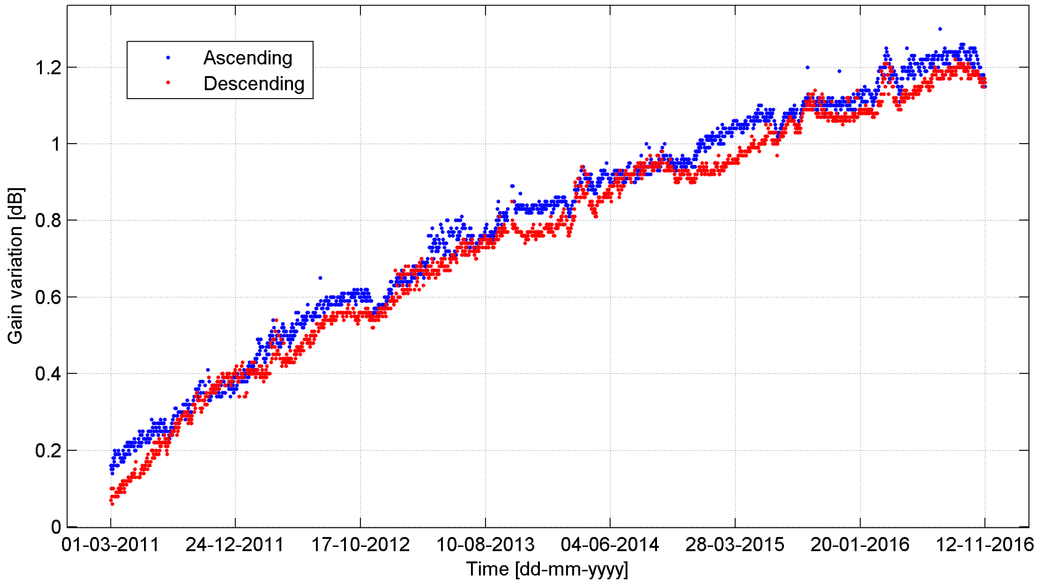

Figure 8: CAL1 SAR gain variation corrections as function of ascending/descending passes over the calibration zone.

In Figure 9 the internal path delay corrections for CAL1 SAR have been processed to remove the increasing trend seen in Table 1 and was smoothed with a running average filter with a length equal to 5 days. By comparing the variations of the internal path delay with the temperature measured by a thermistor placed on the SIRAL antenna bench, it can be noticed that the behaviour of the corrections is roughly anti-correlated with the temperature. Also, the peculiar temperature evolution in CryoSat, which is periodically characterised by high temperature periods (out of eclipse periods) and low temperature periods (eclipse periods), is due to the sun illumination of the spacecraft resulting from the non-sun-synchronous orbit.

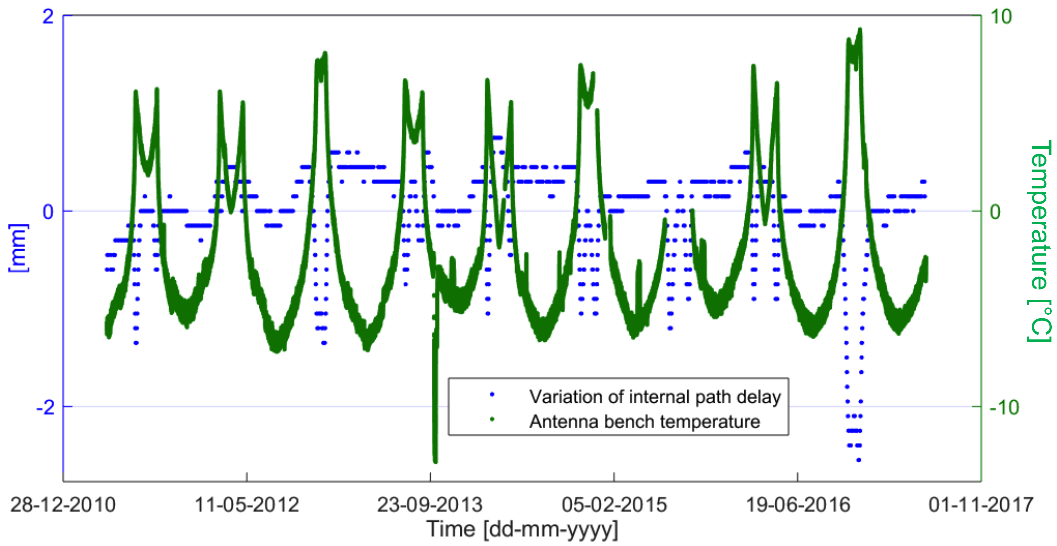

Figure 9: CAL1 SAR internal path delay corrections compared with the temperature of the SIRAL antenna bench.

To clearly describe the stability of SIRAL from the beginning of the mission, Table 1 lists the measured trends for CAL1 calibration corrections. It can be noticed that the pulse-to-pulse calibration corrections are very stable for all the modes and that limited trends are observed for gain variation and path delay.

CAL1 mode	**Internal Path delay**	**Gain variation**	**Pulse-to-Pulse amplitude**	**Pulse-to-Pulse phase**
LRM	0.007 mm/ month	0.015 dB/ month	not applicable	not applicable
SAR	0.035 mm/ month	0.017 dB/ month	negligible	negligible
SARIn Rx1	0.030 mm/ month	0.017 dB/ month	negligible	negligible
SARIn Rx2	0.018 mm/ month	0.018 dB/ month	negligible	negligible

Table 1. Measured trends in CAL1 calibration corrections from November 2010 to November 2016.

For what concerns the range impulse response parameters, the average values and the measured trends on the peak-to-side lobe ratio and on the -3 dB width have been listed in Table 2. It can be noticed that the average values for the range impulse response parameters are in line with the system requirements and that limited trends have been observed.

	Peak-to-Side Lobe Ratio (PSLR)		**-3 dB Width**	
System requirements	-12 dB < PSLR < -16 dB		0.39 m < -3 dB width < 0.44 m	
CAL1 mode	Average Value [dB]	Trend [dB/month]	Average Value [m]	Trend [mm/month]
LRM	13.01	-0.0011	0.420	-0.009
SAR	12.94	0.0002	0.420	0.004
SARIn Rx1	12.95	-0.0001	0.417	-0.002
SARIn Rx2	13.19	-0.0014	0.414	-0.013

Table 2. Measured average values and trends in CAL1 range impulse response quality parameters from November 2010 to November 2016.

3.3 External Calibration with the Svalbard Transponder

3.3.1 Background

ESA deployed a transponder for the CryoSat project. It is a refurbished ESA transponder developed for ERS-1 altimeter calibration, and is deployed at the Kongsberg Satellite Services (KSAT) Svalbard Satellite station, called SvalSAT, as showed in Figure 10.

Figure 10: Transponder and the radome where it is installed.

The transponder is used to calibrate SIRAL's range, datation, and interferometric baseline (or angle of arrival) to meet the mission requirements. In these calibrations three different types of data are used: the raw Full Bit Rate (FBR) data, the stack beams before they are multi-looked (stack data) in the L1B processor, and the L1B data itself. Ideally the comparison between (a) the theoretical values provided by the well-known target, and (b) the measurement by the instrument to be calibrated, provides us with the error the instrument is introducing when performing its measurement. When this error can be assumed to be constant regardless of the conditions, it will provide the bias of the instrument. If the measurements can be repeated after a certain period of time, this can also provide an indication of the instrument drift. The full methodology and the results are described Garcia-Mondejar et al. (2017, this issue). We provide hereafter a synthesis of the main results.

3.3.2 Material and Methods

There are some differences in the algorithms for the modes. In the LRM, the SIRAL echoes are incoherently averaged on-board. In the SAR and SARIn modes, the individual echoes are saved as complex waveforms (I and Q) and the data is sent to ground in the 'time domain', whereas in LRM, the data is sent to ground in the 'frequency domain' after the on-board fast

Fourier transform. In SARIn mode, there are two different echoes, one for each receiving path of the interferometer.

Within the CryoSat processing chain for the SAR and SARIn modes there are different output products for the science data. The FBR product is an intermediate output of the L1B processing chain. The complex waveforms should be fully calibrated (including both instrumental gains and calibration corrections) and aligned in range within each burst. The time tag is given at the surface, i.e. when the middle of the burst reaches the surface. L1A is the starting point for the SAR processing which provides high-resolution products. The L1B Stack data product contains information about the Doppler beams. They are associated to a given surface location, which is formed through the selection of all the beams that illuminate this location, and that contribute to each L1B waveform. Beams are the result of applying Doppler processing to the waveform bursts that allow the conventional altimeter footprint to be divided into a certain number of strips, and thus creating a delay Doppler map. This enables contributions coming from different strips to be identified and collected separately. When all the contributions from different bursts are collected, a stack is formed.

The stack waveforms are provided in I/Q samples (complex waveform) in the frequency domain. The L1B SAR product must contain the same variables as the L1B Stack product, except for the waveform and the stack characterisation parts. A L1B waveform is the average of each stack and is provided in I2Q2 samples (power waveform, computed as the cross product of the complex waveform, the square root of I squared plus Q squared, simplified to I2Q2) in the frequency domain (range domain). Due to the nature of this L1B data (waveforms that have been multilooked, leading to a single waveform per record), there is only one data record (or waveform) that corresponds to the transponder position. The dedicated data processing performed for calibration with the transponder, for the SAR and SARIn echoes, is performed using a dedicated processor developed at ESA. For the LRM, the L1B is directly used as shown in Figure 11.

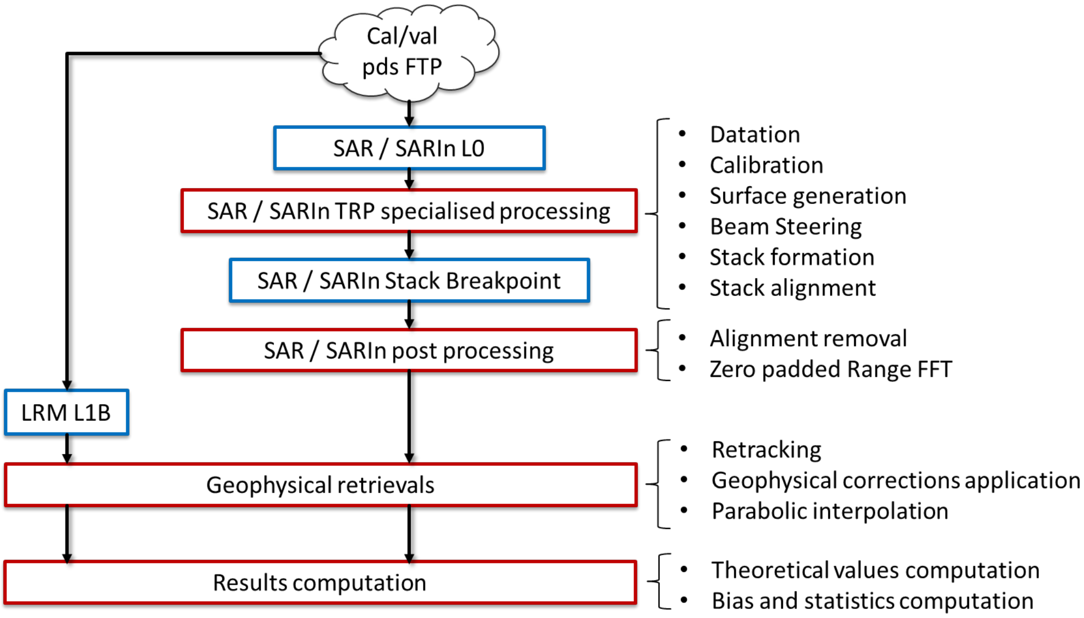

Figure 11: Block diagram with the steps followed to retrieve the results.

After retrieving the L1B Stack products, the range cell migration or slant range correction is undone. With the beams aligned, the moment of maximum approach could not be seen, although the beam with maximum power could be identified. The datation error is also better retrieved when the range is presented as a parabola. A retracking process is then performed in order to determine the epoch. After that, the uncorrected range is computed as described in the CryoSat Product Handbook, in section 2.8 (Bouzinac, 2102):

$$Range_{meas\ uncorr} = \left[win_{delay} + \left(range_{sample} - \frac{N}{2} \right) \cdot \frac{1}{BW} \right] \cdot \frac{c}{2} \qquad (1)$$

where win_{delay} is the two-way time between the pulse emission and the reference point at the centre of the range window (in seconds), N is the number of samples of the waveform, BW is the pulse bandwidth (in Hz or 1/s), c is the speed of light (in m/s), and $range_{sample}$ is the epoch obtained by the retracking method (sample index from 0 to N).

Then the geophysical corrections: the Dry Tropospheric Correction, the Wet Tropospheric Correction, the Ionosphere Correction, the Ocean Loading Tide, the Solid Earth Tide and the

Geocentric Polar Tide, are combined and applied to the range. In addition to the listed corrections present in the product, the ground motion of the Svalbard area is needed in order to compensate for the +8.9 mm/year variation, as shown in Figure 12.

$$Range_{meas} = Range_{meas\ uncorr} + Geo_{corr} \qquad (2)$$

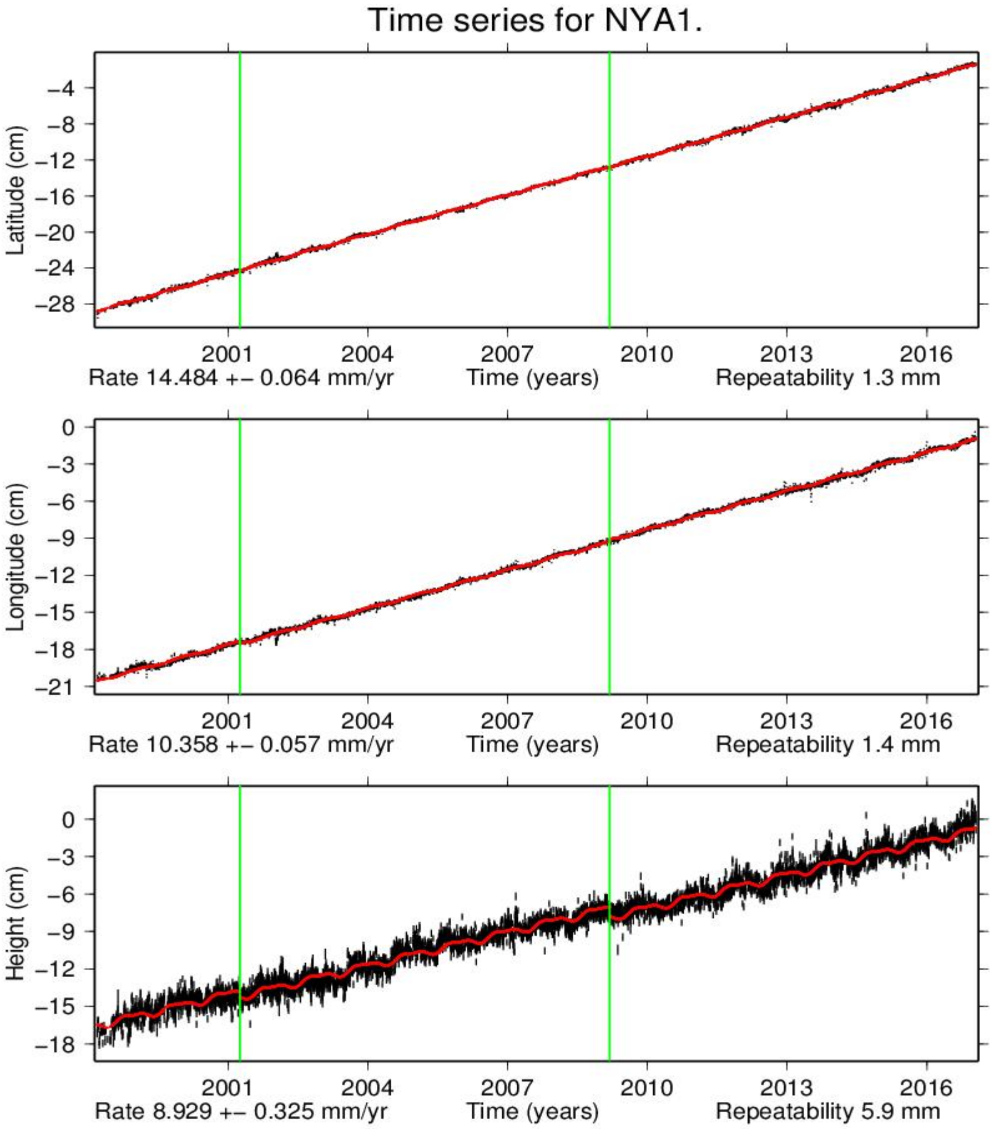

Figure 12: Terrain motion in Ny-Ålesund, close to the Svalbard transponder location computed by the Network for the Detection of Atmospheric Composition Change, NDACC – NOAA (http://www.ndsc.ncep.noaa.gov).

The theoretical range is computed by simply obtaining the distance from the transponder to the SIRAL location for each beam or waveform (in the case of LRM):

$$Range_{theo} = \sqrt{(x_{sat} - x_{TRP})^2 - (y_{sat} - y_{TRP})^2 - (z_{sat} - z_{TRP})^2} \quad (3)$$

Where the satellite and the transponder positions are in Earth-Centred, Earth-Fixed coordinate system.

In SARIn mode, the theoretical angle of arrival can be computed simply by geometry following:

$$\Phi_{theo}(t) = \sin^{-1}\left(\frac{d_0}{r(t)}\right) \quad (4)$$

Where d_0 is the distance from the transponder position to the closest point of the ground track, r(t) is the distance from the satellite location to the transponder position and Φ is the across-track angle (the angle between the nadir direction and the line from the satellite to the transponder position).

The measured angle of arrival in SARIn is obtained from the retracked phase difference waveform with:

$$\Phi_{meas}(t) = \sin^{-1}\left(\frac{\lambda \cdot \Delta phase(t)}{2\pi \cdot B}\right) - roll \quad (5)$$

where λ is the wavelength of the radar signal equal to 0.022084 m, B is the distance between the two antennas equal to 1.1676 m, and Δphase is the retracked phase difference in radians, varying for every measurement.

3.3.3 Results

The results for the range bias are shown in Figure 13a; they have been ordered chronologically in order to evaluate the deviation of the bias. A summary of the statistics is shown in Table 3 Looking at the slope of the regressions, the bias is less than a 1 mm/year drift for SARIn mode. After the correction of the biases found in Baseline-A and B, due to the LRM gate shift, an incorrect platform centre of mass reference and the wrong input parameters in the Instrument Processing Facility Data Base, the range biases in Baseline-C for all three mode have been reduced to less than 4 cm overall and can be considered residuals.

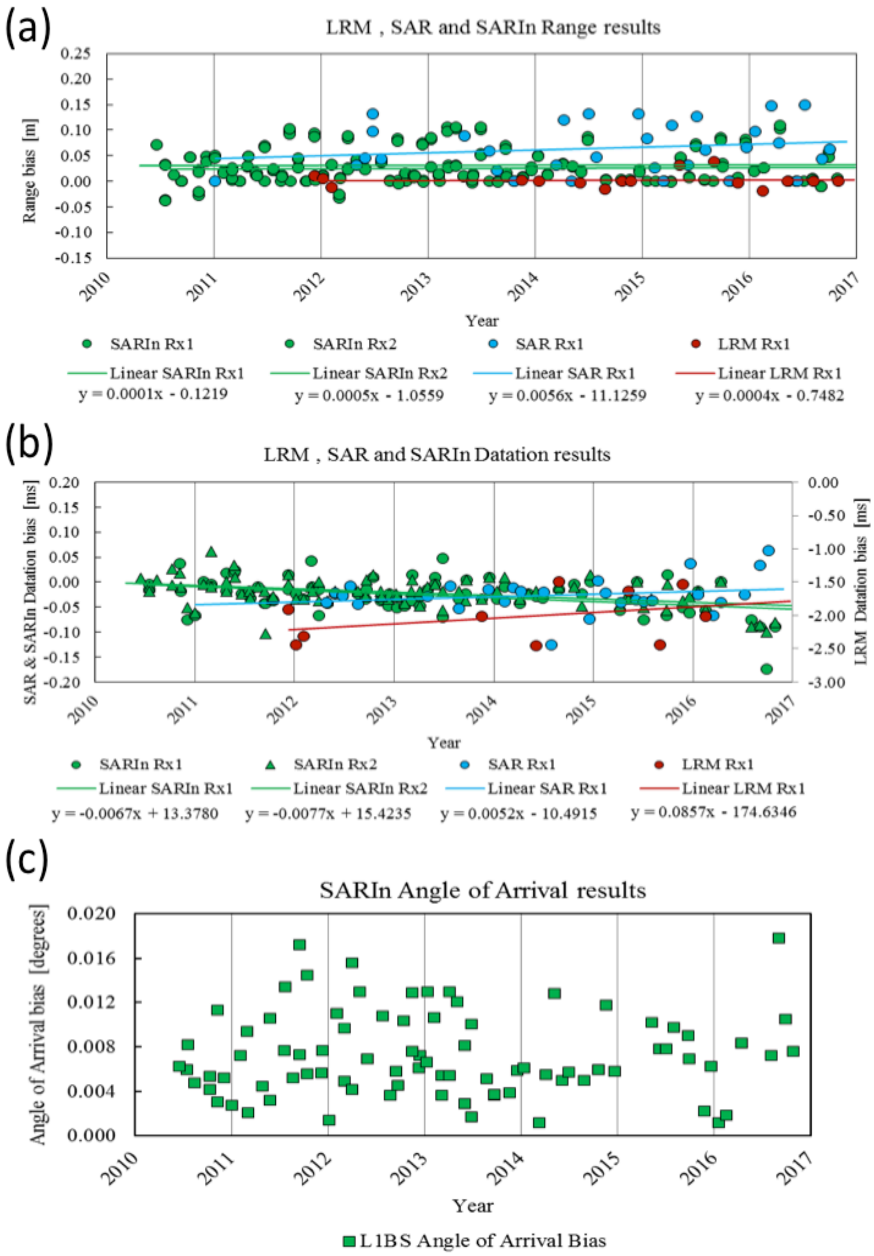

Figure 13: a) Range results over time and regression lines for all modes and separated reception chains. b) Datation results over time and regression lines for all modes and separated reception chains c) Angle of arrival results.

Mode	# of Measurements	Bias	Std	Drift
LRM	10	3.6 mm	19.1 mm	0.4 mm / year
SAR	26	78.8 mm	41.1 mm	5.6 mm / year
SARIn Rx1	87	32.5 mm	32.9 mm	0.1 mm /year
SARIn Rx2	87	31.1 mm	32.6 mm	0.5 mm /year
Overall	210	36.3 mm	37.3 mm	1.5 mm / year

Table 3. Summary of range results

The results for the datation bias are shown in Figure 13b. The results for SAR and SARIn have been referenced to the left vertical axis and the LRM results to the right. The slope of the regressions shows a variation around -6 μs/year. A summary of the datation results is detailed in Table 4. After the correction of the datation biases found in Baseline-A and B, the datation can be considered negligible in SAR and SARIn. The datation trend of around -6 μs/year is related to the motion northward. As the coordinates for the transponder position are fixed during the processing of all passes, the datation error should be varying according to the movement of the terrain in that direction. The correction added in equation (2) only takes into account the height component of the terrain motion.

Mode	# of Measurements	Bias	Std	Drift
LRM	10	-2.025 milliseconds	0.382 milliseconds	+101.2 μs / year
SAR	26	-26.0 microseconds	34.5 microseconds	+5.2 μs / year
SARIn Rx1	87	-24.2 microseconds	33.4 microseconds	-6.7 μs /year
SARIn Rx2	87	-21.2 microseconds	27.7 microseconds	-7.7 μs /year
Overall (SAR/SARIn)	200	-23.2 microseconds	31.1 microseconds	- 6.0 μs / year

Table 4. Datation Results Summary

The results for the Angle of Arrival are shown in Figure 13c and summarized in Table 5. The 0.0072 degree bias is translated at L2 into a geolocation misplacement across track of around 90 m. The standard deviation of 0.0037 degrees is translated into an uncertainty of around 46

m. The requirement for the Angle of Arrival error is 0.0083 degrees, so the results are within the mission requirements.

Mode	# of Measurements	Bias	Std
SARIn	87	0.0072 degrees	0.0037 degrees

Table 5 Angle of Arrival results (SARIn Mode)

3.4 Level 2 Ice Data Quality Analysis

3.4.1 Background

The Department of Space and Climate Physics at the Mullard Space Science Laboratory (MSSL) of UCL supports the development of operational software for the CryoSat ground segment and provides the Ice processing chains required for generating L2 and L2i products, including specialised algorithms supporting the SIRAL instrument's SAR and SARIn measurement modes. The group provides support to ESA as an Expert Support Laboratory in the operational phase of the CryoSat mission and has implemented an operational monitoring and quality analysis service for the CryoSat mission. Data has been monitored since the start of the operational phase (18th Oct 2010). Results are displayed at: http://cryosat.mssl.ucl.ac.uk/qa/.

3.4.2 Material and Methods

MSSL monitors CryoSat performance from L2 data products provided by the ESA Payload Data Segment at Kiruna. Key sea ice and land ice parameters are assessed from the L2 and L2i products. Monitoring L2i parameters provides additional lower level information, which can be useful for verification of the standard L2 products. Key parameters include sea ice and ice sheet elevations, sea ice freeboard, ocean elevations and associated parameters. Associated auxiliary and geophysical correction data, and quality flags are also monitored.

Measuring the elevation residual at orbit crossover points is a primary method of assessing the performance of the altimeter and the processing chain. Crossover height differences are produced for each 30-day data take. The crossover positions and epochs are estimated at the crossing of two linear fits through four measurement locations along the ascending and descending tracks. Points with insufficient data are then rejected. Altimeter height residuals along both passes are filtered and interpolated with a quadratic polynomial at the crossover locations. Apart from sea level change, crossover differences expose errors in the applied range corrections, tide models or orbit altitude. The root-mean-square (RMS) of the crossover differences is a measure of cumulative height error.

For each Polar Region and SIRAL mode, a RMS crossover residual is calculated without the use of geophysical or ionospheric corrections. Corrections are then successively added and the effect on the RMS is plotted. Secondly, for each data, a plot of fully corrected RMS is shown along with the RMS once each correction has been removed and reversed. The reversal is used to check that the sign of the correction is correct. When a correction is reversed, the RMS should increase more than when it is not applied, which therefore gives further insight into the effectiveness of the correction (Figure 14).

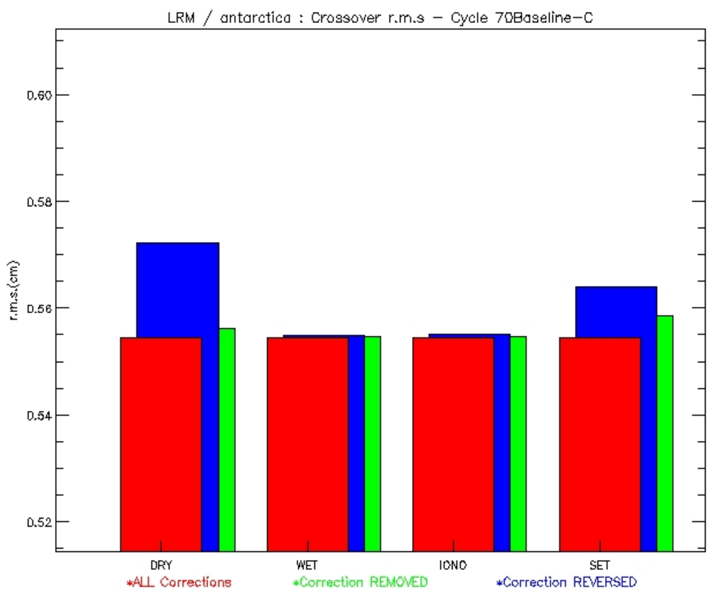

Figure 14: Crossover RMS from LRM over Antarctica (18/06/2016 to 17/07/2016) showing the effects of adding and reversing corrections (dry and wet tropospheric correction, ionospheric correction, and solid earth tide).

3.4.3 Results

Following the implementation of updated Baseline-C Ice processing chains (see Section 2.2), the L2 products were reprocessed back to the start of the mission. MSSL performed quality analysis on the new Baseline-C products to assess the new features and improvements over Baseline-B. Similarly, Baseline-B reprocessed products were assessed against the previous baseline. Parameter plots from each baseline, from the beginning of the mission can be used to quantitatively assess the improvements at each processing chain release. For example, Figure 15 plots the mean bias output from crossover analysis and demonstrates the improvements with each successive baseline using LRM data over the land ice area of Antarctica. Mean time tag biases in Baseline-A, Baseline-B and Baseline-C average, over the data processed by that baseline, are at 6.05 ms, 4.42 ms and -1.04 ms respectively. This represents a 27% improvement of Baseline-B compared to Baseline-A, and 83% improvement of Baseline-C compared to Baseline-A. The time tag bias is computed using the method described in Schutz et al. (1982)). A positive time tag bias indicates that the time stamping of measurements is late while negative values indicate that the time tags are systematically early.

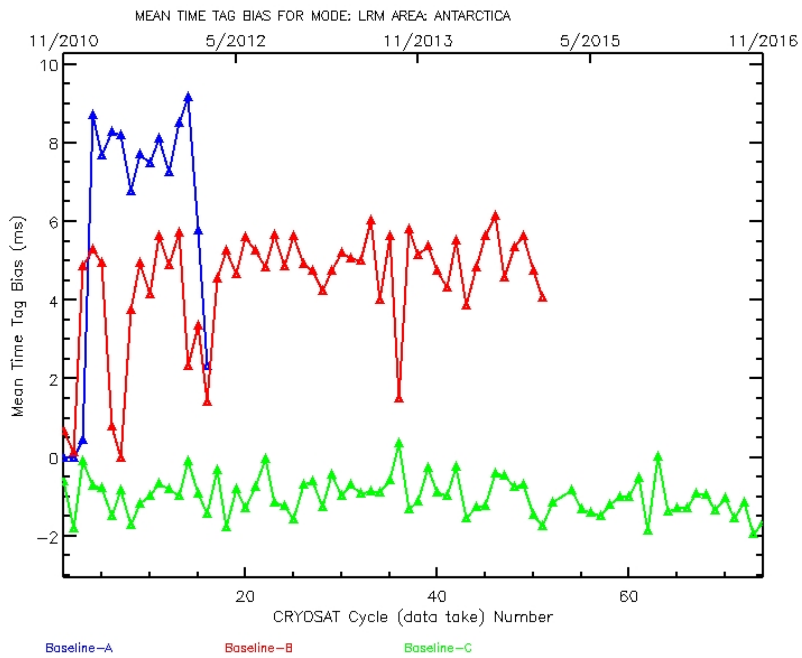

Figure 15: Comparison of mean time tag bias at each processing baseline since the beginning of mission, using LRM data over Antarctica.

In Baseline–C, the combined effect of the L1B and L2 Ice processing upgrades results in significant improvements to the product quality compared to previous releases, and marks the integration of new fields within the products. Both are confirmed to have positive impacts on the scientific exploitation over land ice and sea ice.

Over sea ice, results of analysis at MSSL indicate that Baseline-C freeboard values are coherent and the expected geographical distribution of sea ice thickness is seen. Freeboard from CryoSat L2 data was compared with freeboard from a different processing chain executed at the Centre for Polar Observation and Modelling (CPOM). Some results are reported in the ESA Technical Document (Bouffard et al., 2015). Systematic quality assurance performed at MSSL shows that CryoSat L2 freeboard values continue to be consistent with sea ice thickness and volumes produced by CPOM (available at the CPOM Data Portal: http://www.cpom.ucl.ac.uk/csopr).

A more thorough analysis is expected with the results from ESA's CryoVal Sea Ice project (see http://cryosat.mssl.ucl.ac.uk/cryoval/about-right.html). The CryoVal Sea Ice project is focused on addressing the error budgets for sea ice by making use of extensive in-situ, airborne and satellite datasets acquired in multi-year sea ice regions. Sea ice thicknesses retrievals require numerous processing steps to convert the altimeter's range measurements first to ice freeboard and then to thickness. Each of these steps can introduce uncertainties in the resulting thickness estimate, each requiring careful validation. Preliminary results from the CryoVal Sea Ice Project were presented at North American CryoSat Science Meeting, in Banff, Canada (Haas et al., 2017). Various studies have used a range of coincident submarine and airborne ice thickness observations for validation of CryoSat thickness retrievals from Baseline-C-based products at spatial and temporal scales of ≥10000 km^2 and ≥1 month, respectively. These show correlation coefficients of 0.6-0.8 and RMS errors of 0.3-0.6 m between CryoSat and other thickness retrievals.

Over land ice areas, both the OCOG and CFI retrackers for LRM have been refined, leading to improved retracker performance in Baseline-C, with fewer results being flagged. The mean RMS difference at crossovers has decreased from 0.423 m to 0.418 m for respectively the OCOG retracker in Baseline-B and Baseline-C (Figure 16). Moreover, the percentage of data being flagged as bad by the CFI, Land Ice Retracker and OCOG retrackers has reduced by 1.05%, 5.59% and 15.14% respectively, compared to Baseline-B (Figure 17). Thus, the new Land Ice Retracker provides a good alternative to the existing CFI retracker with an algorithm that can be tuned and further developed to increase performance in the future.

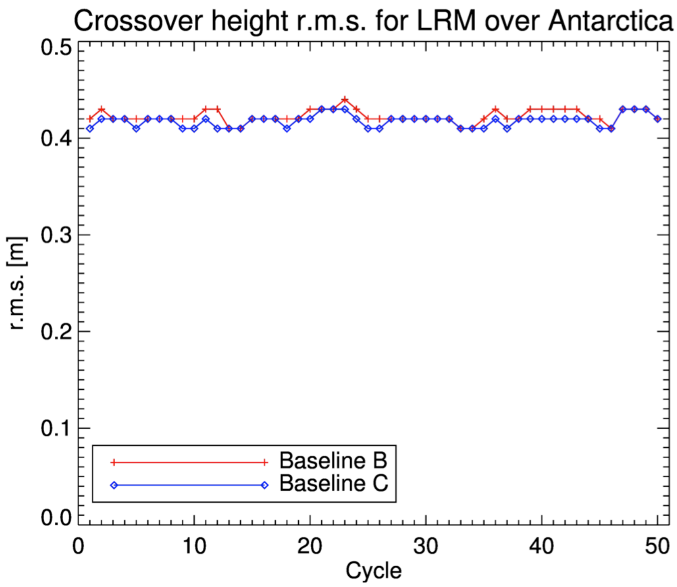

Figure 16: LRM Crossovers showing mean height RMS (m)

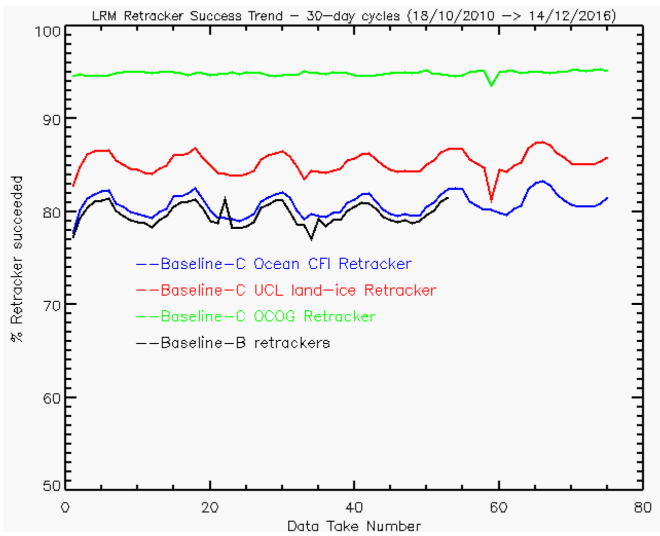

Figure 17: LRM Retracker success rate: trend since beginning of mission

In addition to routine quality analysis, validation of CryoSat L2 data over ice sheets has been also performed by several ESA-funded projects and individual studies. The ESA CryoVal Land Ice Project, which aims to quantify the error sources and accuracy of CryoSat data over land ice, has done an extensive comparative analysis in which CryoSat absolute elevation data from each Baseline-C retracker has been evaluated against airborne (Ice Bridge Airborne

Topographic Mapper) and in-situ data over the Greenland ice sheet. It has yet to issue its final report but early results released at the ESA Living Planet Symposium in 2016 (Sorenson et al., 2016) indicate an accuracy at the 10-15 cm RMS level with little bias, dependent on retracker selection, surface slope and volume penetration effects. The ESA Climate Change Initiative projects for the Antarctic and Greenland ice sheets (2015-2018) have independently performed validations of the absolute elevation and surface elevation change rates derived from CryoSat L2 elevation data as compared with Ice Bridge Airborne Topographic Mapper data and found mean accuracy levels of 10 cm and derived surface elevation change rate accuracy of less than 1 m/year in all ice sheet basins. Ice Bridge surveys are predominantly in areas of the ice sheet margins where slopes are highest and so accuracy over the whole ice sheet is likely to be significantly better. Other studies over the interior of East Antarctica (e.g. Schröder et al., 2016) showed that the new Baseline-C processor improved the observation quality over the flat ice sheets by comparison with global navigation satellite system ground surveys.

Recent investigations based on interferometric swath processing from CryoSat SARin data, also confirm good performance. This technique operates by unwrapping the interferometric phase of the SARIn echoes over sloping ice sheet surfaces (Hawley et al., 2009), resulting in a wide swath of elevation measurements across track, providing up to two orders of magnitude more elevation measurements than the point-of-closest-approach alone (Gourmelen et al., 2016). This technics allows up to 10 times finer resolution mapping of the elevation change of glaciers in the Antarctic and Greenland margins (Figure 18) and new capabilities to measure changes in small ice caps and sub-glacial lakes. Recent studies (Gourmelen 2017, *personal communication*) have shown that the improvements implemented in Baseline-C, such as the doubling of the range window to 240 m, a new star tracker processor and the recent correction of the roll bias (Scagliola et al., 2017, this issue), have led to a significant increase in the number of elevations that extended swath processing is able to deliver and have shown lower noise levels in the waveform’s leading edge (see Figure 19).

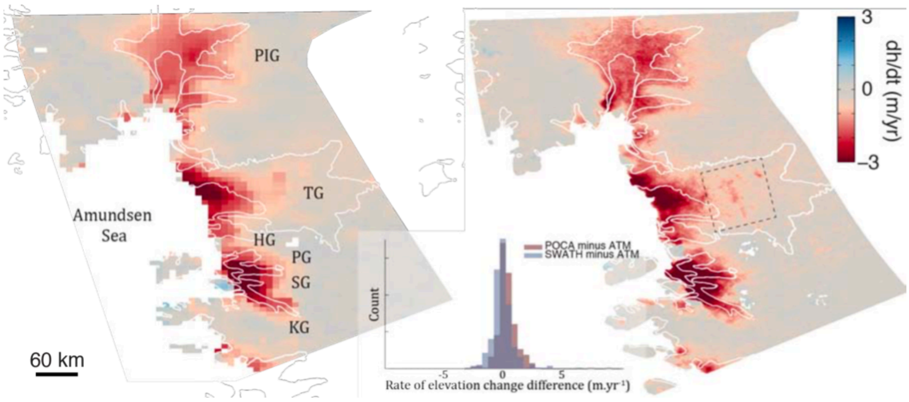

Figure 18: Surface elevation change over the Amundsen Sea Sector of West Antarctica, mapped with 10 km grid spacing (left) from conventional point-of-closest approach altimetry processing and at 500 m from CryoSat swath processing (right) (Gourmelen 2017, *personal communication*).

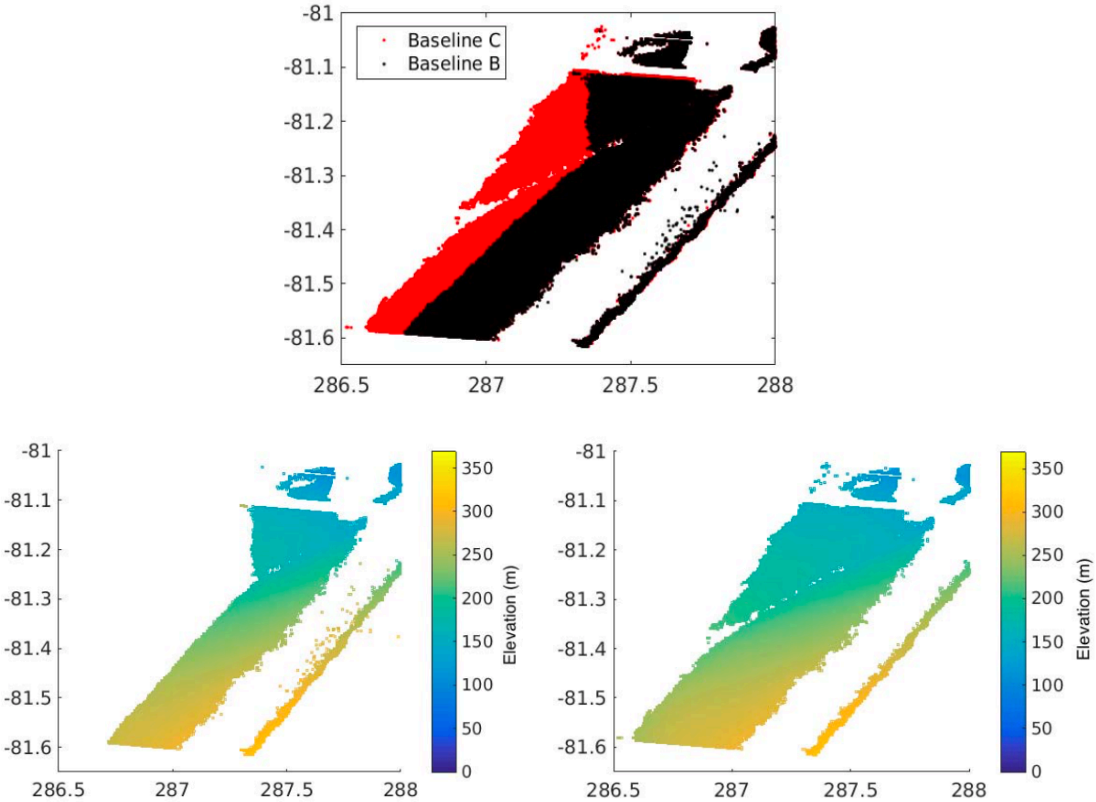

Figure 19: CryoSat swath elevation from Baseline-C (bottom right) and Baseline-B (bottom left) and overlay (top) show the increase in elevation measurements provided by the new Baseline-C (Gourmelen 2017, *personal communication*).

4 Known Baseline-C Limitations and Planned Evolutions

A continual process of improvement and tuning of retracking schemes and auxiliary models is followed between baseline releases; mainly based on the outcomes from the scientific literature and Research & Development projects (e.g. Land ice and Sea ice CryoVal ESA projects). Despite the good Baseline-C results over land ice and sea ice, there are planned evolutions to fix anomalies and further improve CryoSat ice products in the future, including the switch from ESA Earth Explorer format to the more convenient NetCDF format. Many of these changes will fall under the next Ice processing chain upgrade, Baseline-D. Below is a high level picture of the main changes; further technical details can be found in Mannan (2017).

During the interferometric calibration analysis, it was observed that the Star Tracker selection performed on-board the satellite and followed by the Star Tracker processor does not always give the best possible performance. It was recommended that the methodology for this selection strategy be reviewed, taking into account the temperature information of the different thermistors placed in the antenna bench.

Regarding the L1B products, it is planned to correct the window delay for the drift of the Ultra Stable Oscillator (USO) frequency with respect to the nominal frequency, while in the current products this correction is left to the users. Additionally, it is planned that the on-ground algorithm to compute the mispointing angles will be improved as described in Scagliola al. (2017, this issue) to increase the quality of the pitch, roll and yaw information.

Over sea ice, the freeboard results can be improved by correcting for the effect of overlying snow. At present, in Baseline-C, this correction is left to the L2 product users to perform, although the obsolete Warren snow-depth climatology (Warren, 1999) is provided as a starting point. The incorporation of up-to-date information on snow cover in future baselines, and the provision of a correction to freeboard, will increase the L2 product quality. In addition, investigations are on going for further refinements of the SAR retracking and lead-detection methods (e.g. Passaro et al., 2017; this issue) with the objective to reduce the signal-to-noise ratio of the freeboard value.

Over land ice, a particular target for Baseline-D is to investigate whether updates can be made to the slope and ambiguity-detection models to use more recently created DEMs. Moreover, a prototype processor has been developed to produce calibrated Pseudo-LRM waveforms from SARIn FBR processing in preparation for a potential switch to SARIn mode over the interior of the Antarctic or Greenland ice sheets. This aims to provide time-series continuity between LRM and SARIn acquisitions, and therefore ice volume and elevation.

The CryoSat L2 processing chain is optimised for operation over the cryosphere. The results over other surfaces may therefore be sub-optimal when compared to results from other missions designed to target those surfaces. For example, the SARIn chain currently has a height bias when the surface type is closed sea or land. Changes can be made to the processing scheme that will allow improved operation over other surfaces, such as inland water, without impacting results from the primary mission targets. Some options for such changes will be explored during the implementation of Baseline-D.

5 Conclusions and Perspective

Following the switch to the Baseline-C Ice processors, significant improvements have already been observed in the Baseline-C L1B and L2 products, relative to the previous Baseline-B products. The ESA quality control and validation activities have demonstrated that most of the known issues in the previous Ice Baseline-A and Baseline-B have been resolved in Baseline-C.

The continuous monitoring of the SIRAL internal calibration corrections has revealed the stability of the instrument up to November 2016. In particular, the performance of the instrument in terms of range resolution has not changed from the beginning of the operational phase. Only a minor decrease in the signals-to-noise ratio is expected due to the increasing gain variation correction, however this does not impact the system requirements. The dependence of the SIRAL instrument behaviour on its thermal status has also been verified in order to better understand the relationship between the Calibration 1 corrections and solar illumination, and to optimise the calibration plan in future by better considering the thermal effects on SIRAL. Dedicated calibration campaigns have been planned for full orbits and the corresponding calibration corrections will be analysed.

Regular analyses at the Svalbard transponder show that the different biases from the previous Ice Baseline-A and Baseline-B have been corrected. Regarding the long-term drift, the external calibration results confirm that the performance of the CryoSat altimeter is very stable, as demonstrated by internal calibration analysis and quality assessment activities over the ocean (Bouffard et al. 2017, this issue). Although the main purpose of the external calibration is to determine the long-term deviation of the external paths, this activity has been essential to resolve anomalies in the different processing Baselines. Currently, the Crete transponder (Mertikas et al., 2016) is being used for that purpose. Further analysis will be performed with CryoSat data and it will be used to validate the Sentinel 3A and 3B studies over the same targets.

Quality analysis of the CryoSat ice products also confirms performance over the sea ice and land ice domains, consistent with the initial mission requirements despite some limitations and known issues, which will be fixed in the next processing baseline. These future processing algorithm and format upgrades will aim to maximise the uptake and use of CryoSat data by scientific users by facilitating the on-going measurement of regional and basin-scale changes in the thickness of sea ice and the elevation of ice sheets and mountain glaciers.

References

Bamber, J. L., Gomez-Dans, J. L., and Griggs, J. A., 2009. A new 1 km digital elevation model of the Antarctic derived from combined satellite radar and laser data – Part 1: Data and methods, *The Cryosphere*, 3, 101–111.

Bouffard, J., M. Naeije, E. Schrama, C. J. Banks, F. M. Calafat, P. Cipollini , H. M. Snaith, E. Webb, A. Hall, R. Mannan, P. Féménias and T. Parrinello, 2017. CryoSat Ocean: Product Quality Status and future Evolution. Submitted to: "The CryoSat Satellite Altimetry Mission: 7 years of scientific exploitation" special issue of *Advances in Space Research* (this issue).

Bouffard, J., R. Mannan, and D. Brockley, 2015. *Level 2 product evolutions and quality improvements in Baseline C*. Version 3, *IDEAS+/ESA, XCRY-GSEG-EOPG-TN-15-00004*, available at: https://earth.esa.int/documents/10174/1773005/C2-Evolution-BaselineC-Level2-V3.

Bouzinac, C., 2012. *CryoSat Product Handbook*. ESA, available at: https://earth.esa.int/documents/10174/125272/CryoSat_Product_Handbook.

Brown, G., 1977. The average impulse response of a rough surface and its applications. *IEEE Transactions on Antennas and Propagation,* 25, 67-74, doi: 10.1109/TAP.1977.1141536.

Calafat, F. M., P. Cipollini, J. Bouffard, H. Snaith, and P. Féménias, 2017. Evaluation of new CryoSat products over the ocean. *Remote Sensing of Environment*, 191, 131-144, doi: 10.1016/j.rse.2017.01.009.

Cullen, R., D. J. Wingham, P. Viau, C. R. Francis, and C. Mavrocordatos, 2007. ESA's CryoSat-2 multi-mode level 0 to level 1b science processors – algorithm design and prelaunch verification with the Airborne Advanced Synthetic Interferometric Radar Altimeter System (ASIRAS). *Proceedings of the 'Envisat Symposium 2007'*, Montreux, Switzerland: ESA, 23-27 April 2007, SP-636.

Fornari, M., M. Scagliola, N. Tagliani, T. Parrinello, and A. G. Mondejar, 2014. CryoSat: SIRAL calibration and performance. *2014 IEEE Geoscience and Remote Sensing Symposium (IGARSS 2014)*, Quebec City, QC, Canada: IEEE, 702-705, doi: 10.1109/IGARSS.2014.6946520.

Garcia-Mondejar, A., M. Fornari, J. Bouffard, P. Féménias, and M. Roca, 2017. CryoSat-2: Range, Datation and Interferometer Calibration with Svalbard Transponder. Submitted to: "The CryoSat Satellite Altimetry Mission: 7 years of scientific exploitation" special issue of *Advances in Space Research* (this issue).

Gourmelen, N., Escorihuela, M.J., Foresta, L., Shepherd, A., Roca, M., Nagler, T., Wuite, J., Muir, A., Baker, S., and D. Brockley, 2016. Swath processing of CryoSat for the Cryosphere. , *4th CryoSat User Workshop*, 9-13 May 2016, Prague, Czech Republic.

Haas C, S. G. Baker, J. Beckers, M. Davidson, S. Farrell, R. Forsberg, S. Gerland, S. Hendricks, S. M. Hvidegaard, J. King, R. Ricker, H. Skourup, and G. Spreen, 2017. Validation of CryoSat Sea Ice Thickness Retrievals. *North-American CryoSat Science Meeting,* Banff, Canada: ESA, 20-24 March 2017.

Hawley, R. L., Shepherd, A., Cullen, R., and Wingham, D. J., 2009. Ice-sheet elevations from across-track processing of airborne in- terferometric radar altimetry, *Geophys. Res. Lett*., 36, L25501, doi:10.1029/2009GL040416.

Mannan, R., 2017. *CryoSat Ice Data Quality Status Summary*. ESRIN, Frascati, Italy: ESA, available at: https://earth.esa.int/documents/10174/129120/CryoSat_IPF_anomalies.

Mertikas, S. P., C. Donlon, C, Mavrocordatos, I. N. Tziavos, D. Galanakis, A. Tripolitsiotis, X. Frantzis, O. Andersen, 2016. Calibration and Validation of SWOT Oceanographic Products Using Gavdos & Crete Permanent Infrastructure. *SWOT Science Team Meeting,* Pasadena, CA, USA: NASA, 13-16 June 2016.

Parrinello, T., Shepherd, A., Bouffard, J., Badessi, S., Casal , T., Fornari M., Maestroni, E., and Scagliola, M., 2017. CryoSat: ESA's ice Mission - Seven Years in Space. In "The CryoSat Satellite Altimetry Mission: 7 years of scientific exploitation" Special Issue of *Advance in Space Research* (this issue).

Passaro, M., Muller, F.L, and Dettmering, D., 2017. Lead detection using Cryosat-2 delay-doppler processing and Sentinel-1 SAR images. *In press* in "The CryoSat Satellite Altimetry Mission: 7 years of scientific exploitation" Special Issue of *Advance in Space Research* (this issue). http://dx.doi.org/10.1016/j.asr.2017.07.011

Rey, L., P. de Chateau-Thierry, L. Phalippou, C. Mavrocordatos, and R. Francis, 2001. SIRAL, a high spatial resolution radar altimeter for the CryoSat mission. *2001 IEEE Geosciencce and Remote Sensing Symposium (IGARSS'01),* Sydney, NSW, Australia: IEEE, 3080–3082, doi: 10.1109/IGARSS.2001.978261.

Ridout, A., 2014. *New Mean Sea Surface for the CryoSat-2 L2 SAR Chain*. Issue 1.0, UCL/ESA, C2-TN-UCL-BC-0003, available at: https://wiki.services.eoportal.org/tiki-download_wiki_attachment.php?attId=3609&page=CryoSat%20Technical%20Notes&download=y

Scagliola, M., M., Fornari, J. Bouffard, and T. Parrinello, 2017. The CryoSat interferometer: end-to-end calibration and achievable performance. Submitted to: "The CryoSat Satellite Altimetry Mission: 7 years of scientific exploitation" special issue of *Advances in Space Research* (this issue).

Scagliola, M, and M. Fornari, 2015. Main evolutions and expected quality improvements in Baseline C Level 1b products. Issue 1.3, Aresys/ESA, C2-TN-ARS-GS-5154, available at: https://earth.esa.int/documents/10174/1773005/C2-BaselineC_L1b_improvements_1.3.

Scagliola, M., M. Fornari, J. Bouffard and T. Parrinello, 2016. CryoSat SIRAL: instrument performance after 5 years of operations. *2016 Living Planet Symposium*, Prague, Czech Republic: ESA, 9-13 May 2016, SP-740, 316-320.

Schröder, L., Richter, A., Fedorov, D. V., Eberlein, L., Brovkov, E. V., Popov, S. V., Knöfel, C., Horwath, M., Dietrich, R., Matveev, A. Y., Scheinert, M., and Lukin, V. , 2017. Validation of satellite altimetry by kinematic GNSS in central East Antarctica, The Cryosphere, 11, 1111-1130, https://doi.org/10.5194/tc-11-1111-2017, 2017.

Schutz, B. E, B. D. Tapley, and C.K. Shum, 1982. Evaluation of the SEASAT Altimeter Time Tag Bias. *Journal of Geophysical Research: Oceans,* 87 (C5), 3239-3245, doi: 10.1029/JC087iC05p03239.

Skourup, H., S. Farrell, S. Hendricks, R. Ricker, T. Armitage, A. Ridout, O. B. Andersen, C. Haas, and S. G. Baker, 2017. An Assessment of the State-of-the-Art Mean Sea Surface and Geoid Models of the Arctic Ocean: Implications for Sea Ice Freeboard Derivation. Submitted to: *Journal of Geophysical Research: Oceans*.

Sørensen, LS, Baker, S, Csatho, B, Forsberg, R, Gourmelen, N, Helm, V, Langley, K, Martinez, B, Nienow, P, Schrama, E, Shepherd, A, Davidson, M & Simonsen, SB, 2016. CryoSat Land Ice Product Validation within the CryoVal-LI project. ESA Living Planet Symposium 2016, Prague, Czech Republic, 09/05/2016 - 13/05/2016.

Warren, S. G., I. G. Rigor, N. Untersteiner, V. F. Radionov, N. N. Bryazgin, Y. I. Aleksandrov, and R. Colony (1999), Snow depth on Arctic sea ice, *J. Clim.,* 12(6), 1814–1829.

Wingham, D. J., Francis, C. R., Baker, S., Bouzinac, C., Brockley, D., Cullen, R., de Chateau-Thierry, P., Laxon, S. W., Mallow, U., Mavrocodatos, C., Phalippou, L., Ratier, G., Rey, L., Rostan, F., Viau, P., and Wallis, D. W., 2006. CryoSat: A mission to determine the fluctuations in Earth's land and marine ice fields. *Adv. Space Res.,* 37 (4), 841–871, doi: 10.1016/j.asr.2005.07.027.